Bioorganic & Medicinal Chemistry xxx (2016) xxx–xxx

Contents lists available at ScienceDirect

Bioorganic & Medicinal Chemistry

journal homepage: www.elsevier.com/locate/bmc

Phosphonate-based irreversible inhibitors of human γ-glutamyl transpeptidase (GGT). GGsTop is a non-toxic and highly selective inhibitor with critical electrostatic interaction with an active-site residue Lys562 for enhanced inhibitory activity

Akane Kamiyama [a,†], Mado Nakajima [a,‡], Liyou Han [a,§], Kei Wada [b], Masaharu Mizutani [a,¶], Yukiko Tabuchi [a,‖], Akiko Kojima-Yuasa [c], Isao Matsui-Yuasa [c], Hideyuki Suzuki [d], Keiichi Fukuyama [e,††], Bunta Watanabe [a,*,‡‡], Jun Hiratake [a,*,‡‡]

[a] Institute for Chemical Research, Kyoto University, Gokasho, Uji, Kyoto 611-0011, Japan
[b] Organization for Promotion of Tenure Track, University of Miyazaki, 5200 Kihara, Kiyotake, Miyazaki 889-1692, Japan
[c] Department of Food and Human Health Sciences, Graduate School of Human Life Science, Osaka City University, 3-3-138 Sugimoto, Sumiyoshi-ku, Osaka 558-8585, Japan
[d] Division of Applied Biology, Graduate School of Science and Technology, Kyoto Institute of Technology, Goshokaido-cho, Matsugasaki, Sakyo-ku, Kyoto 606-8585, Japan
[e] Department of Biological Sciences, Graduate School of Science, Osaka University, Toyonaka, Osaka 560-0043, Japan

ARTICLE INFO

Article history:
Received 17 June 2016
Revised 25 August 2016
Accepted 27 August 2016
Available online xxxx

Dedicated to Professor Jun Hiratake who deceased after he submitted the original manuscript

Keywords:
γ-Glutamyl transpeptidase
Phosphonate diesters
GGsTop
Mechanism-based inhibitor
Electrostatic interaction
Active-site residue Lys562
Selectivity
Cytotoxicity

ABSTRACT

γ-Glutamyl transpeptidase (GGT, EC 2.3.2.2) that catalyzes the hydrolysis and transpeptidation of glutathione and its *S*-conjugates is involved in a number of physiological and pathological processes through glutathione metabolism and is an attractive pharmaceutical target. We report here the evaluation of a phosphonate-based irreversible inhibitor, 2-amino-4-{[3-(carboxymethyl)phenoxy](methoyl)phosphoryl}butanoic acid (GGsTop) and its analogues as a mechanism-based inhibitor of human GGT. GGsTop is a stable compound, but inactivated the human enzyme significantly faster than the other phosphonates, and importantly did not inhibit a glutamine amidotransferase. The structure–activity relationships, X-ray crystallography with *Escherichia coli* GGT, sequence alignment and site-directed mutagenesis of human GGT revealed a critical electrostatic interaction between the terminal carboxylate of GGsTop and the active-site residue Lys562 of human GGT for potent inhibition. GGsTop showed no cytotoxicity toward human fibroblasts and hepatic stellate cells up to 1 mM. GGsTop serves as a non-toxic, selective and highly potent irreversible GGT inhibitor that could be used for various in vivo as well as in vitro biochemical studies.

1. Introduction

γ-Glutamyl transpeptidase (GGT, EC 2.3.2.2) is a heterodimeric enzymes found widely in organisms from bacteria, plants to mammals and plays a central role in glutathione metabolism by catalyzing the hydrolysis and transpeptidation of glutathione (γ-L-glutamyl-L-cysteinylglycine) and its conjugates.[1,2] GGT is the extracellular enzyme and catalyzes the cleavage of the γ-glutamyl amide bond of glutathione by a modified ping-pong mechanism via a γ-glutamyl-enzyme ester intermediate to transfer the γ-glutamyl group to water (hydrolysis) or amino acids and peptides (transpeptidation) (Scheme 1A).[2–5]

* Corresponding authors. Tel.: +81 774 38 3233 (B.W), +81 774 38 3231 (J.H.).
E-mail addresses: bunta@scl.kyoto-u.ac.jp (B. Watanabe), hiratake@scl.kyoto-u.ac.jp (J. Hiratake).
† Present address: Seiwakasei Co., Ltd, 5-9-19 Nakaishikiri-cho, Higashiosaka, Osaka, Japan.
‡ Present address: Shionogi Pharmaceutical Research Center, SHIONOGI & CO., LTD, 1-1, Futaba-cho 3-chome, Toyonaka, Osaka 561-0825, Japan.
§ Present address: Institute for Liberal Arts and Sciences, Kyoto University, Japan.
¶ Present address: Graduate School of Agricultural Science, Kobe University, 1-1 Rokkodai, Nada-ku, Kobe 657-8501, Japan.
‖ Present address: Wakayama Research Center, Kao Corporation, 1334 Minato, Wakayama 640-8580, Japan.
†† Present address: Department of Applied Chemistry, Graduate School of Engineering, Osaka University, Suita, Osaka 565-0871, Japan.
‡‡ Equally contributed.

http://dx.doi.org/10.1016/j.bmc.2016.08.050
0968-0896/

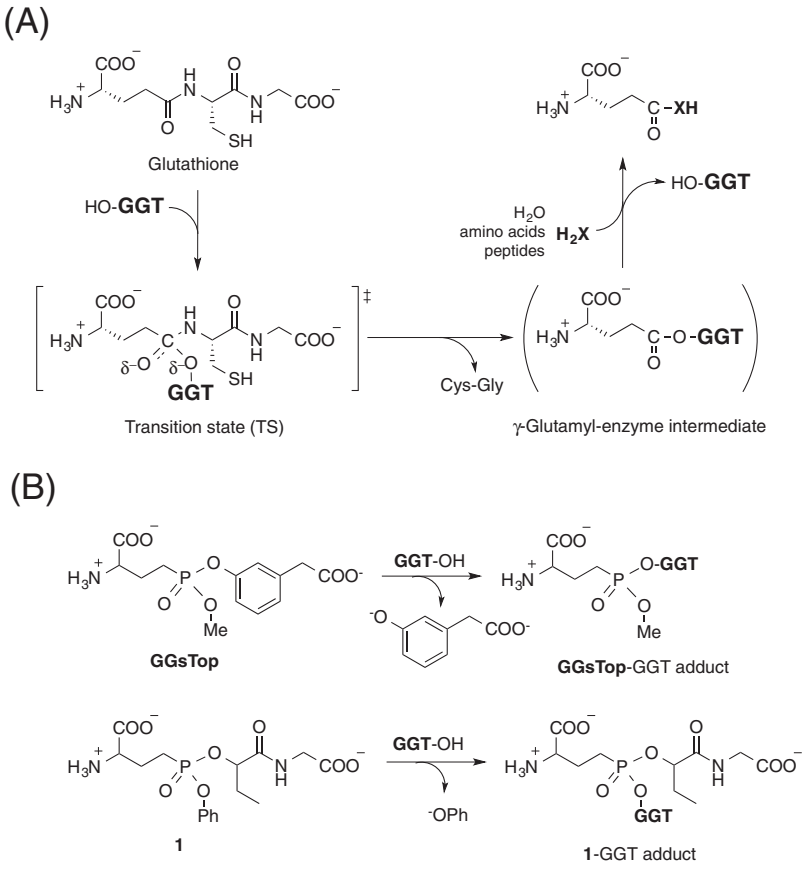

Scheme 1. Proposed catalytic mechanism of GGT (A), and proposed mechanism of GGT inactivation by GGsTop and peptidyl phosphonate **1**[46] (B).

GGT plays a pivotal role in glutathione homeostasis as the sole extracellular enzyme that cleaves the γ-glutamyl bond of glutathione; GGT initiates the hydrolysis of extracellular glutathione as a critical step in providing cells with cysteine, the limiting substrate for intracellular *de novo* synthesis of glutathione.[1,6–8] GGT is also involved in the metabolism of xenobiotics by cleaving the γ-glutamyl bond of glutathione-*S*-conjugates in the first step in their detoxication.[9,10] The physiological reaction catalyzed by mammalian GGT is regarded as the hydrolysis of glutathione,[1,10–12] but regardless of hydrolysis or transpeptidation, GGT certainly functions as a critical enzyme for supplying cells with cysteine for enhancing glutathione biosynthesis. Accordingly, the overexpression of GGT is often observed in human tumors[13–17] to cope with increased oxidative stress. The roles of GGT in tumor progression,[18,19] growth acceleration[20,21] and the expression of such malignant phenotypes as drug resistance[20,22,23] and metastasis[24,25] have been suggested repeatedly.

GGT is also implicated in many physiological disorders such as neurodegenerative diseases,[26–28] diabetes,[29,30] cardiovascular disease,[31–34] and pulmonary disease.[35,36] Hence the serum GGT level has been used extensively as a diagnostic/prognostic marker of liver dysfunction, coronary heart diseases, type 2 diabetes, stroke, and atherosclerosis.[1,34] While GGT is recognized as an integral component of cellular antioxidative defense system,[1,8,23] several lines of evidence have indicated that GGT promotes oxidative stress by producing Cys-Gly, a highly reactive thiol that generates reactive oxygen species (ROS) via a metal ion-catalyzed reduction of molecular oxygen.[37] Therefore, GGT is also recognized as a pro-oxidant enzyme that potentially promotes oxidative stress.[38–43] The implication of GGT in a number of pathological processes strongly suggests a causative role of this enzyme,[37,39,43–45] rather than a simple result of cellular adaptation to oxidative stress.[1,8] Hence, GGT is an attractive pharmaceutical target for cancer chemotherapy and a vast array of physiological disorders involving oxidative stress and glutathione metabolism.[23,25,35]

We previously developed the potent phosphonate-type mechanism based GGT inhibitors (Scheme 1B).[46,47] Among them, 2-amino-4-{[3-(carboxymethyl)phenoxy](methoyl)phosphoryl} butanoic acid (designated GGsTop hereafter) is a simple and stable compound, but strongly inhibits human GGT.[46] We also revealed that human GGT recognizes the negative charge of the C-terminal carboxy group of glutathione by a positively charged key residue located in the Cys-Gly binding site, whereas *Escherichia coli* GGT does not have such a substrate recognition mechanism.[46] Recently, Hu et al. reported that the key residue was Arg520 of *Bacillus anthracis* GGT, that corresponds to Lys562 of human GGT, by computational and kinetic approaches.[48] The result prompted us to further investigate the role of Lys562 of human GGT using phosphonate-based inhibitors as chemical probes. Here we report the synthesis of the GGsTop analogous simple phosphonates **2a–h**, **3a** and **3b** (Fig. 1) and evaluated their inhibitory activities against human and *E. coli* enzymes to probe the active site structures. In parallel with the structure–activity relationships, we made a complex crystal of GGsTop with *E. coli* GGT, molecular modeling, and sequent alignment to estimate the residues that might be critical for human GGT for affinity to GGsTop. Site-directed mutagenesis of human GGT of the possible residue revealed that the active-site residue Lys562 was indeed the critical residue that electrostatically interacted with GGsTop for enhancing its activity. The selectivity, stability and toxicity data of GGsTop are also reported.

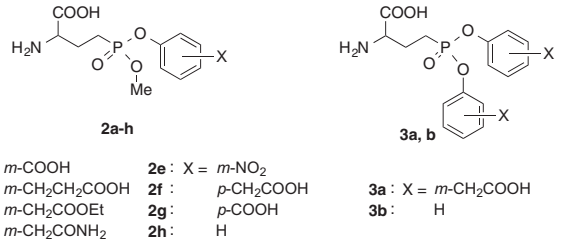

2a : X = *m*-COOH
2b : *m*-CH_2CH_2COOH
2c : *m*-CH_2COOEt
2d : *m*-CH_2CONH_2
2e : X = *m*-NO_2
2f : *p*-CH_2COOH
2g : *p*-COOH
2h : H

3a : X = *m*-CH_2COOH
3b : H

Figure 1. Structure of the GGsTop-analogous phosphonate inhibitors **2a**–**h**, **3a**, and **3b**.

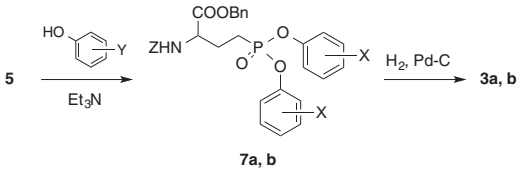

7a : Y = *m*-CH_2COOBn
7b : H

Scheme 3. Synthetic route of inhibitors **3a** and **3b**.

2. Results

2.1. Selection of GGsTop analogues

Compounds **2c**, **2d**, and **2e** were selected to evaluate the type of interaction (electrostatic, hydrogen-bonding and/or both) between the enzyme and the inhibitor. The rest (**2a**, **b**, **f**, **g**, **h**) were designed to discuss the interaction of the terminal carboxylate from a topological point of view. Compounds **3a** and **3b** are double substituted phenyl esters to see if the enzyme accommodates the bulky diphenyl phosphonate diesters. We synthesized each inhibitor as a mixture of four stereoisomers, arising from the stereogenic centers on the α-carbon of the glutamate moiety and the phosphorus atom. Though we have not obtained clear evidence whether the inhibitory activity of the one stereoisomer of the GGsTop analogues is inhibited/enhanced by the other stereoisomers, we have successfully established the structure–activity relationship of the benzene ring of GGsTop using racemic inhibitors.[46] Therefore, we expected that the racemic inhibitors in this study are useful chemical probes for the assessment of the electrostatic role of Lys562 in the mechanism of substrate recognition.

2.2. Synthesis

The hetero-diester inhibitors **2a**–**h** were synthesized according to the previous report (Scheme 2).[46,47]

Briefly, racemic benzyl 2-benzyloxycarbonylamino-4-(dihydrxyphosphoryl)butanoate (Z-APBA-OBn **4**)[46] was converted to the corresponding dichloride **5**. This compound was reacted successively with one equivalent of methanol and the respective phenol derivative in the presence of triethylamine to give the protected precursors **6a**–**h**. Benzylic protecting groups of **6a**–**d** and **6f**–**h** were removed under catalytic hydrogenation condition to afford the desired inhibitors **2a**–**d** and **2f**–**h**. In the case of **6e**, benzylic protecting group was removed by $AlCl_3$/anisole to avoid the reduction of the nitro group. Treatment of the dichloride **5** with two equivalents of phenol derivatives gave the homo-diesters **7a** and **7b**, which were converted to **3a** and **3b**, respectively, by hydrogenolysis (Scheme 3).

2.3. Inactivation of human and *E. coli* GGT by synthetic inhibitors

The inhibitory activities of the synthetic phosphonate derivatives toward human and *E. coli* GGT were measured and evaluated as described.[46,49] Since all the inhibitions are irreversible in nature, the inhibitor potency was evaluated by k_{on} values, the 2nd order rate constant for the reaction between the inhibitor and the enzyme.[49] The results are summarized in Table 1.

The trend of human GGT inactivation by the phosphonate analogues was interesting and greatly different from that of *E. coli* GGT inactivation. Human GGT was inactivated specifically faster by GGsTop, but not by other structurally similar analogues: simple truncation (**2a**) or elongation (**2b**) by a methylene unit reduced the activity significantly. Removal of the negative charge (**2c** and **2d**) resulted in a significant decrease in activity, although the latter has a hydrogen bonding donor/acceptor ability. Topology of the carboxylate was also important; the *p*-CH_2COOH (**2f**) and *p*-COOH (**2g**) did not contribute to the affinity with the enzyme active site and reduced the activity as compared GGsTop. Compound **2e** (*m*-NO_2) is worth noting. This compound inactivated human GGT to the same extent as GGsTop, but this is simply because of the presence of a good leaving group of *m*-nitrophenol (pK_a = 8.36).

It is noteworthy that a homo-diester of *m*-carboxymethylphenol **3a** showed potent inhibitory activity, while a homo-diester of simple phenol **3b** exhibited only weak inhibitory potency. The effect of the introduction of a carboxymethyl group on the *meta* position was similar for both the hetero- and the homo-diester, and resulted in 100 to 130 times increase of inhibitory activity (GGsTop vs **2h** and **3a** vs **3b**). These results strongly suggested that a positively charged amino acid resides in the specific position in the Cys-Gly-recognizing site of human GGT and recognized the C-terminal carboxylate of the inhibitors.

In contrast, the inhibitory trend of the synthetic inhibitors on *E. coli* GGT well correlated to the leaving group ability of phenols (the pK_a value of phenols) (Broensted plot, data not shown). These results suggested the loose recognition of the phosphonate inhibitors by *E. coli* GGT, which is correlated to the large k_{on} values for all the inhibitors as compared to those with human GGT.

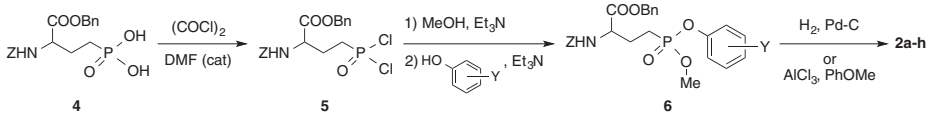

6a : Y = *m*-COOBn
6b : *m*-CH_2CH_2COOBn
6c : *m*-CH_2COOEt
6d : *m*-CH_2CONH_2
6e : Y = *m*-NO_2
6f : *p*-CH_2COOBn
6g : *p*-COOBn
6h : H

Scheme 2. Synthetic route of inhibitors **2a**–**h**.

Table 1
Inhibitory activities of GGsTop, **2a–h**, **3a** and **3b** toward human and *E. coli* GGT

Inhibitor	Leaving group 		k_{on}[a] [M^{-1} s^{-1}]	
	X	pK_a	Human GGT	*E. coli* GGT
GGsTop[b]	*m*-CH_2COO^-	9.71[c]	51 ± 3	150 ± 10
2a	*m*-COO^-	9.14[c]	1.6 ± 0.1	450 ± 30
2b	*m*-$CH_2CH_2COO^-$	10.1[c]	7.7 ± 0.5	71 ± 2
2c	*m*-CH_2COOEt	9.75[c]	1.2 ± 0.1	120 ± 10
2d	*m*-CH_2CONH_2	9.89[c]	1.9 ± 0.1	400 ± 30
2e	*m*-NO_2	8.36	49 ± 3	5100 ± 700
2f[b]	*p*-CH_2COO^-	9.84[c]	0.33 ± 0.01	210 ± 10
2g	*p*-COO^-	8.70[c]	5.2 ± 1.4	3200 ± 500
2h[b]	H	9.98	0.40 ± 0.03	120 ± 10
3a	*m*-CH_2COO^-	9.71[c]	40 ± 1.3	Not determined
3b	H	9.98	0.41[d]	27.8[d]
Acivicin[e]	—[f]	−6.18	0.40 ± 0.02	4210 ± 10

[a] Second-order rate constants for enzyme inactivation.
[b] Ref. 46.
[c] Calculated pK_a values using Advanced Chemistry Development (ACD/Labs) Software V8.14 for Solaris (©1994–2006). Calculated pK_a values of the corresponding methyl ester for **2a**, **2b**, **2f**, **2g**, and **3a**.
[d] Error limit was not determined due to duplicate measurements.
[e] Ref. 49.
[f] The leaving group is HCl.

2.4. Effect of GGsTop on glutaminase activity of asparagine synthetase

Acivicin is a classical and has been the most popular irreversible inhibitor of GGT.[21,25] However, acivicin is not selective and inhibits many glutamine-dependent biosynthetic amidotransferases,[50] to show potent cytotoxicity and neurotoxicity.[51,52] In this study, we evaluated the effect of acivicin and GGsTop toward the glutaminase activity of asparagine synthetase B, a typical glutamine-dependent amidotransferase, to examine the selectivity of GGsTop (Fig. 2). Acivicin (0.1 mM) facilely inactivated glutaminase activity, whereas GGsTop did not inhibit glutaminase activity even at 10 mM.

2.5. X-ray crystallography of *E. coli* GGT in complex with inhibitor 1 and assignment of Lys562 as the probable residue for the recognition of negative charge at C-terminal of GGsTop

We recently reported the crystal structures of *E. coli* GGT in complex with azaserine and acivicin, and revealed the mechanism of recognition of the γ-glutamyl moiety of glutathione and catalytic process in detail.[53] More recently, human GGT in complex with GGsTop was reported.[54] In this structure, the C-terminal of GGsTop was lost as a leaving group when GGsTop formed a covalent bonding with the catalytic threonine, and thus there is no clue for the initial structure with respect to the residues to the C-terminal of the intact GGsTop. When we conducted our study, we could not access the large amount of recombinant human GGT for crystallization. Therefore we used *E. coli* GGT for crystallization in complex with the inhibitor **1**[46] (Scheme 1B) to solve the crystal structure to see the possible Cys-Gly binding site, although the *E. coli* enzyme appears to have a loose active site without a specific positively charged residue (Table 1). The results are shown in Figure 3 (PDB ID: 5B5T). As expected from our previous X-ray structural study,[55] the observed electron density of the γ-glutamyl moiety was sufficiently clear, while only weak electron density was observed for the Cys-Gly moiety. In Figure 3A, the most probable structure of **1** in the substrate binding pocket of *E. coli* GGT is depicted as a stick model. The model suggests that *E. coli* GGT does not recognize the Cys-Gly moiety of **1** strictly, although the γ-glutamyl moiety is recognized precisely. The cavity for the accommodation site for the Cys-Gly moiety of **1** mainly charged neutral or negative (Fig. 3B, colored in grey or red), and accordingly a neutral amino acid residue such as Ser572 might correspond to the residue. Figure 3C shows a probable **1** binding structure in human GGT model around the substrate binding pocket, which model was constructed from the crystal structure of human GGT in complex with GGsTop (PDB ID: 4ZBK). The human GGT model thus constructed gave a more positive charge than that of *E. coli* GGT and two possible positively charged part, the protonated residue of Lys562 or Lys181 (as human GGT numbering, patch 1 and 2). From the distance of 3–8 Å and 13–18 Å for patch 1 and patch 2, respectively, to the C-terminal carboxy group, we concluded that the patch 1 (Lys562) might be the key residue that recognized the negative charge of the C-terminal of the inhibitor.

Another remarkable point is that the multiple sequence alignment exhibits that Lys562 of human GGT was conserved among rat and *Helicobacter pylori* and replaced by another basic amino acid arginine in the case of *Pseudomonas aeruginosa* (Fig. 4). A neutral serine (Ser572) resides at this position in *E. coli* GGT, though. The absence of a basic residue and the presence of a small neutral Ser residue at this site explain the absence of negative charge recognition and loose selectivity for the phosphonate inhibitors of *E. coli* GGT (Table 1).

These data strongly suggested that Lys562 of human GGT is the key residue for the recognition of the negatively charged GGsTop.

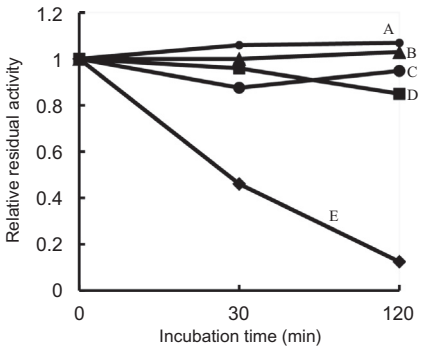

Figure 2. Inhibition of glutaminase activity of *E. coli* asparagine synthetase B by acivicin and GGsTop. (A) 0.1 mM of GGsTop. (B) 1.0 mM of GGsTop. (C) 10 mM of GGsTop. (D) No inhibitor. (E) 0.1 mM of acivicin.

To confirm the hypothesis, we made a mutant human GGT, namely K562S. The N-terminal anchor domain was truncated, and the resulting wild type (WT) enzyme and the mutant enzyme (K562S) were expressed by baculovirus-infected insect cells. It is known that the human GGT protein without the anchor domain is expressed as a soluble enzyme and it exhibits virtually identical enzymatic character to that of human GGT with the anchor domain.[56] The WT human GGT was expressed as a mature protein by autocatalytic processing[57] during the period of infection. The autocatalytic process of K562S mutant was somewhat slow and was not enough under the same conditions, but the successful processing was attained by giving additional processing period for the purification step. Somewhat lower hydrolytic activity of K562S mutant was observed as compared to the WT enzyme (see Table 3).

2.6. Enzymatic activity of WT human GGT and K562S mutant

To evaluate the effect of the mutation on the substrate recognition, we measured γ-glutamyl transfer activity using γ-L-glutamyl-*p*-nitroanilide (γ-Glu-PNA) as a γ-glutamyl donor. Glycylglycine (Gly-Gly) and its methyl ester (Gly-GlyMe), and glyicne methyl ester (GlyMe) were used as an acceptor substrate of γ-glutamyl group. The results are summarized in Table 3.

It should be noted that GGT not only catalyzes the transfer of γ-glutamyl group of γ-Glu-PNA to acceptors, but also hydrolyzes the γ-glutamyl bond of γ-Glu-PNA to give glutamate and *p*-nitroaniline. The enzymatic activity without acceptor (Milli Q) represents the hydrolytic activity. Hence the observed activity in the presence of acceptor molecules in Table 3 is the sum of γ-glutamyl transfer and hydrolytic activity. In the case of WT human GGT, its enzymatic activity greatly increased (by 26 times) when Gly-Gly was

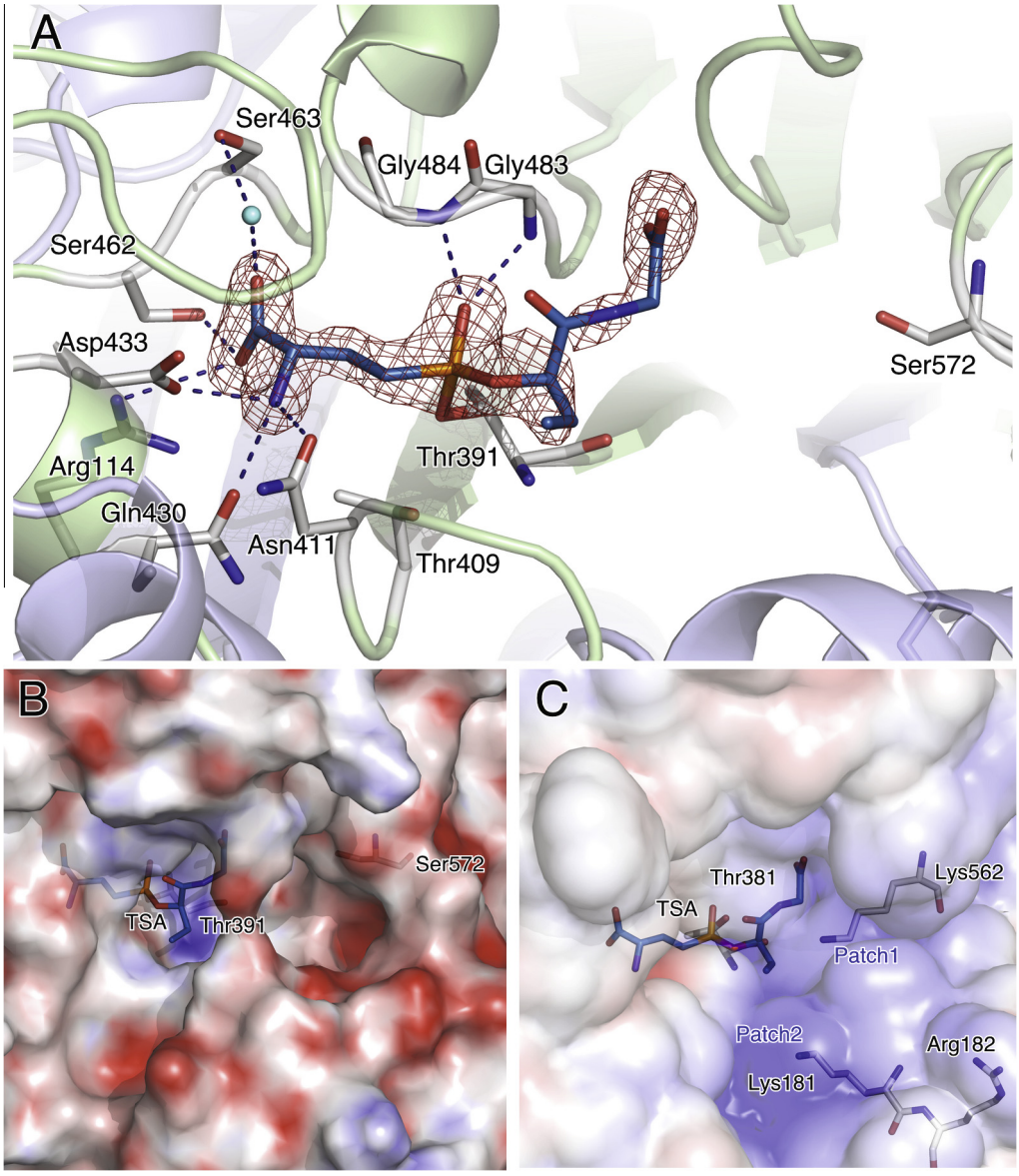

Figure 3. The structure of *E. coli* GGT in complex with peptidyl phosphonate inhibitor **1**. (A) The electron density map of *E. coli* GGT around inhibitor **1**. An $F_o - F_c$ map omitting **1**, contoured at 3.0 σ (red), is overlaid with a stick model of the bound **1**. The most probable structure of **1** was depicted as stick model because of the weak electron density around the Cys-Gly moiety of **1**. (B) Surface drawing of the substrate binding pocket of *E. coli* GGT. Red and blue colors represent negative and positive charge surface potential, respectively. The color scale ranges from −5 kT per electron (red) to +5 kT per electron (blue). The stick model of **1** (TSA), the catalytic residue (Thr391), and Ser572 are shown. (C) The **1** (TSA) binding model in human GGT. This model was generated by the superposing the γ-glutamyl moiety of GGsTop in human GGT (PDB ID: 4ZBK) on that of **1** in *E. coli* GGT. Patch 1 and 2 represents localization of positive charge.

Please cite this article in press as: Kamiyama, A.; et al. *Bioorg. Med. Chem.* (2016), http://dx.doi.org/10.1016/j.bmc.2016.08.050

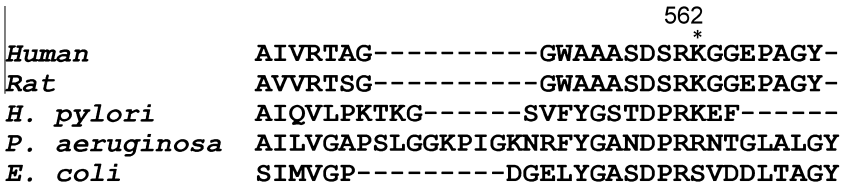

Figure 4. Sequence alignment of GGTs from human, rat, *Helicobacter pylori*, *Pseudomonas aeruginosa* and *E. coli*. Lys562 (numbering of human GGT) is asterisked.

Table 2
Crystallographic parameters of the inhibitor **1**–*E. coli* GGT complex[a]

Crystallographic data	
Space group	$P2_12_12_1$
Cell parameters (Å)	a = 78.1, b = 126.6 c = 129.6
Resolution range (Å)	50.0–1.70 (1.80–1.70)
Observed reflections	639,167
Unique reflections	135,141
Mean $I/\sigma(I)$	99.9 (2.34)
Redundancy	4.7 (3.6)
Completeness (%)	99.9 (82.0)
R_{sym}[b] (%)	5.2 (56.0)
CC(1/2)	99.9 (82.0)
Refinement statistics	
R_{cryst}[c] (%)	17.8
R_{free}[d] (%)	19.4
RMSD from ideal values	
Bond length (Å)	0.007
Bond angle (°)	0.95
Average B-factor (Å^2)	24.0
Ramachandran plot	
Favored (%)	97.48
Allowed (%)	2.34
Outliers (%)[e]	0.19
PDB entry	5B5T

[a] Values in parentheses are for the outermost shell.
[b] $R_{sym} = \Sigma_{hkl}\Sigma_i|I_i(hkl) - \langle I(hkl)\rangle|/\Sigma_{hkl}\Sigma_i I_i(hkl)$, where $\langle I(hkl)\rangle$ is the average intensity over equivalent reflections.
[c] $R_{cryst} = \Sigma||F_{obs}(hkl)| - |F_{calc}(hkl)||/\Sigma|F_{obs}(hkl)|$.
[d] R_{free} is the R value calculated for 5% of the data set not included in the refinement.
[e] Asn411 in the two crystallographically independent molecules.

added as an acceptor. Gly-GlyMe also enhanced the enzymatic activity, but the degree was moderate (4.9 times), and the activity enhancement of GlyMe was marginal. These results clearly indicate the importance of the interaction of negative charge at the C-terminal of acceptors between an active site positive residue probably by Lys562.

In contrast, the K562S mutant, its affinity towards Gly-Gly dramatically decreased (2.0% of WT), whereas it retained hydrolytic activity (45% of WT). Importantly, the K568S mutant did not respond to the addition of any acceptor molecules appreciably; the rate enhancement was less than five-fold. Detailed scrutiny may find the preferred GlyMe as an acceptor, but the extent of rate enhancement was not significant as compared to the WT enzyme. These results clearly show the critical role of Lys562 in human GGT for recognition of the acceptor substrate, and the electrostatic interaction between the positive charge on the side chain of Lys562 and the negative charge on the C-terminal of carboxylate of Gly-Gly (acceptor molecules) is important. Since the acceptor Gly-Gly is very much likely to mimic the Cys-Gly of glutathione, the electrostatic interaction of Cys-Gly and Lys562 moiety is also expected to be critical when glutathione is hydrolyzed in the physiologic reaction. The substitution of Lys562 with Ser (Ser572) in *E. coli* GGT and its broad inhibitor activity (Table 1) suggests that the *E. coli* enzyme is a general hydrolytic enzyme for a wide variety of γ-glutamylamides including glutathione.

Both WT, K562S mutant enzymes and the phosphonate inhibitor GGsTop in hands, we examined the responsiveness of both enzyme towards GGsTop. The progress curves of the time-dependent inhibition are shown in Figure 5. WT human GGT was completely inactivated in 1 min by GGsTop at 1 mM (Fig. 5A), but in contrast, the K562S mutant was significantly less sensitive toward GGsTop and retained ca. >80% activity even after 5 min (Fig. 5B).

These results clearly indicated that GGsTop is a mechanism-based inhibitor that utilizes the electrostatic interaction of its C-terminal *m*-carboxymethyl group. With respect to the k_{on} values of GGsTop and **2h**, the active site Lys562 of human GGT enhances the inhibitory activity of GGsTop by 128-fold (Table 1). Based on the differences of the K_i and the k_{inact} values between GGsTop and inhibitor **2f** we previously reported,[46] the active-site Lys562 is a key residue responsible for promoting accommodation of GGsTop in the active site (42-fold) and facile inactivation of the enzyme (4.2-fold). The electrostatic interaction is topologically strict, and only *m*-carboxymethyl group is recognized. Hence, GGsTop is regarded as an inhibitor that is recognized not only by the γ-glutamyl binding site, but also by the Cys-Gly binding site (Lys562) of human GGT by electrostatic interaction.

2.7. Hydrolytic stability of GGsTop

GGsTop is an active ester of phosphonate. Therefore GGsTop must be sufficiently stable in aqueous solution for use in vitro and in vivo studies. We therefore examined the hydrolytic stability of GGT and its analogues in D_2O with ^{31}P NMR. In a neutral aqueous solution, P–O bond of phenyl ester is cleaved selectively to give monomethyl phosphonate and phenol. Figure 6 depicts the progress of hydrolysis. GGsTop was a stable compound without any hydrolysis observed at neutral and ambient temperature for at least 28 day. Other phosphonates with an alkyl substituent (*p*-CH_2COOH) were also stable. However, the *m*-nitrophenyl

Table 3
Specific hydrolytic and transpeptidation activities of WT and K562S mutant

	Enzymes	Acceptor			
		Milli Q	GlyGly	GlyGlyMe	GlyMe
Specific activity (U/mg)	WT	17.1 ± 0.4	443 ± 4	83.7 ± 0.4	25.0 ± 4.6
	K562S	7.69 ± 0.08	8.73 ± 0.14	11.8 ± 1.0	24.8 ± 0.5
Relative rate (fold)	WT	1	25.9	4.91	1.46
	K562S	1	1.14	1.53	3.22

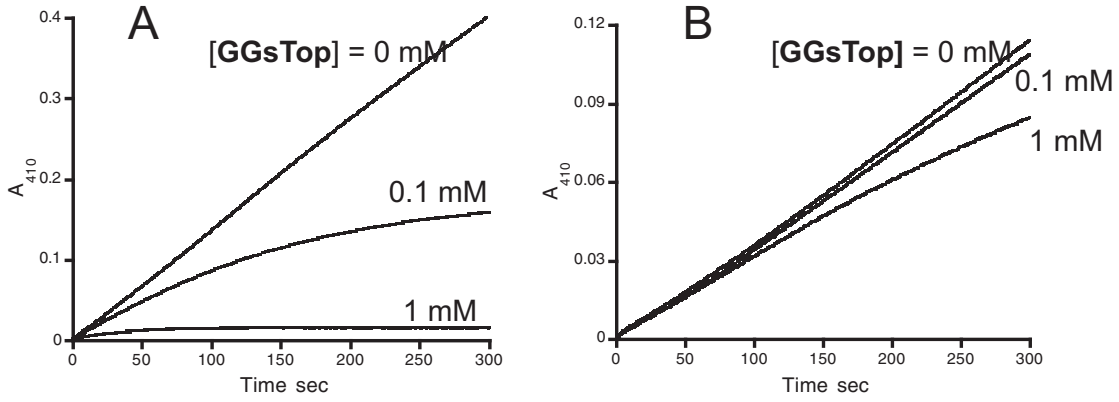

Figure 5. Inhibitory profiles of the WT (A) and K562S mutant (B) human enzymes toward GGsTop. Progress curves are shown for the hydrolysis of γ-glutamyl-*p*-nitroanilide in the presence of GGsTop (0, 0.1 and 1 mM).

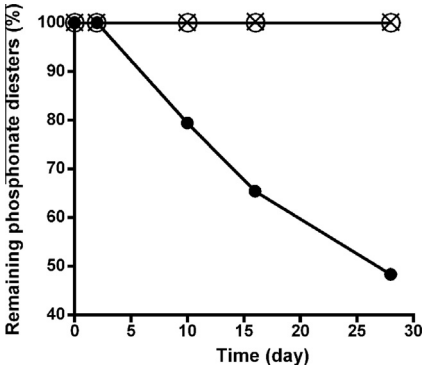

Figure 6. Hydrolytic stability of phosphonate diesters GGsTop (○), **2f** (×) and **2e** (●) determined by ^{31}P NMR in D_2O at 23 °C.

derivative (**2e**) was unstable and hydrolyzed appreciably after 28 day. This is consistent with the high chemical activity of this compound that enabled the inhibition of both human the *E. coli* GGT with high rate (Table 1).

2.8. Cytotoxicity of GGsTop

GGsTop is an active ester of phosphonate and may function as an irreversible inhibitor of unknown hydrolases. We therefore studied the toxicological aspect of GGsTop. We first examined if GGsTop influenced any adverse effect on cultured mammalian cells. Human skin fibroblasts (CCD-1059SK) were incubated with GGsTop (up to 1 mM) for 24 h. After incubation, cell morphology and cell viability was examined. Any concentration of GGsTop was not induced morphological change and cell death (Figs. 7 and 8).

The same results were obtained for rat hepatic stellate cells (Fig. 9). Hence we concluded that GGsTop did not induce cytotoxicity for mammalian cells up to 1 mM.

Furthermore, GGsTop was negative in AMES test and exhibited negative results and no toxicity in in vitro cell growth inhibition and chromosome aberration test using Chinese hamster lung cells (Supplemental Contents S.2. and S.3.). We therefore concluded that GGsTop is a non-toxic and safe compound.

3. Discussion

Structure–activity relationships on GGsTop analogues clearly indicated that the electrostatic interaction of *m*-carboxylmethyl group of the inhibitor was essential for high inhibitory activity toward human GGT. No such special interaction was observed with the *E. coli* enzyme, which is in good agreement with the active site Lys562 is substituted with Ser572. A hydrogen bonding interaction cannot substitute for the electrostatic interaction (**2d**). These results strongly indicated that a specific basic residue was present in the Cys-Gly binding site in human GGT. Interestingly, the topology of the carboxylate was rather strict, and none of the truncation (**2a**) or elongation (**2b**), or *p*-substituted derivatives (**2f** and **2g**) exhibited high activity. It is of interest to see such a strong topological constraint for a charge-charge interaction. As a result, none the GGT analogues surpassed the GGsTop in terms of the inhibition potency toward human GGT. It is worth noting that the sterically hindered *m*-carboxylmethyl diester (**3a**) exhibited almost the same activity as that of the hetero ester GGsTop. Human GGT probably recognizes the negative charge of *m*-carboxymethyl group on one arm, irrespective of hetero- and homo-diester. In the case of more sterically hindered homo-diester, the other *m*-carboxymethylphenyl group might be excluded from the active site, sticking out of the enzyme.

Acivicin is a classical inhibitor of GGT, but it is highly toxic because of inhibition of a broad array of glutamine-dependent amidotransferases. Therefore we examined the selectivity to see if GGsTop inhibits glutaminase activity of asparagine synthetase B. As shown in Figure 2, GGsTop did not inhibit glutaminase activity at all even at 10 mM. GGsTop is probably excluded from the active site of glutaminase due to the presence of sterically hindered *m*-carboxymethylphenyl group, while glutaminase only accommodates smaller glutamine specifically as substrate.

As was expected from the inhibition profile of *E. coli* GGT where the recognition was loose, a loose but a probable model was obtained from the poor electron density at the Cys-Gly binding region (Fig. 3A). From the X-ray structure model of human GGT and the sequence alignment, we estimated a probable residue (Lys562) as the key residue in human GGT. The site-directed mutagenesis of Lys562 of human GGT gave a K562S mutant successfully and its transpeptidation was measured. Whereas the K562S mutant was 45% less active as hydrolase, its transpeptidation activity towards Gly-Gly dramatically decreased (less than 2.0%) than WT. A recent paper demonstrated that mutations of human GGT at this site (K562N, K562Q) greatly diminished the transpeptidation activity.[48] The authors demonstrated clearly that Lys562 was a key residue that interacts with the acceptor substrate (Gly-Gly). Our data are well consistent with their results. Since the acceptor substrate is most likely to mimic the Cys-Gly of glutathione, Lys562 is also most likely an important residue that recognizes the C-terminal carboxy group of glutathione. Finally the mutant K562S mutant was significantly less sensitive towards GGsTop (Fig. 5), indicating that Lys562 is also important in recognizing

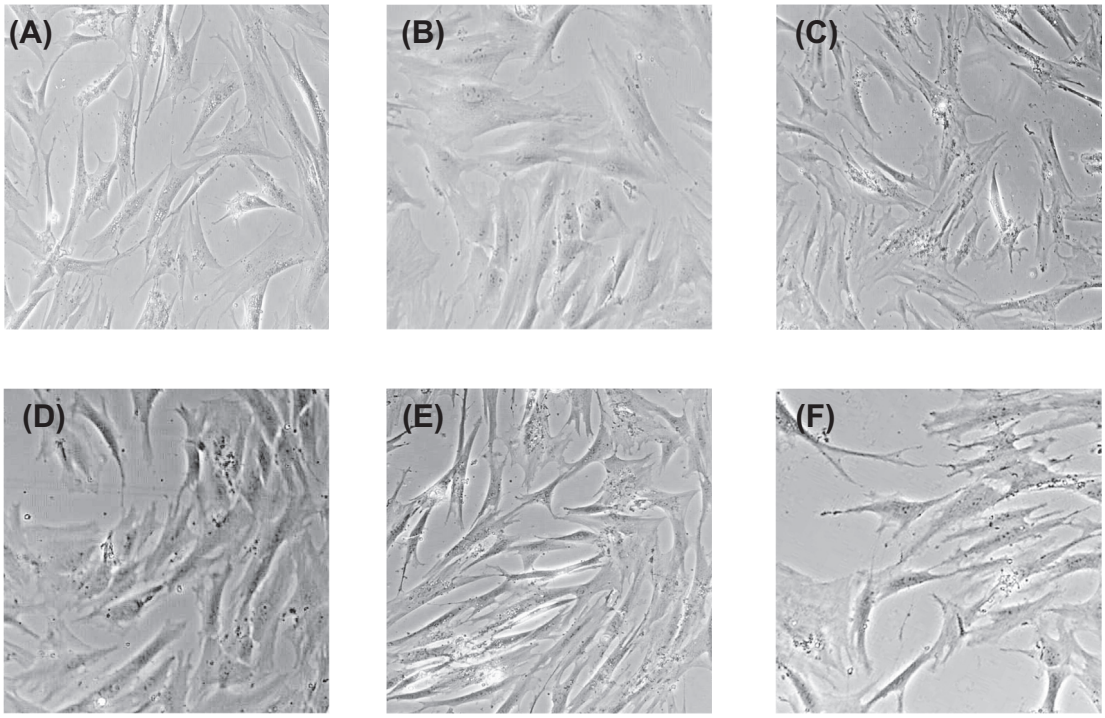

Figure 7. Effect of GGsTop on the morphology of human skin fibroblasts (CCD-1059SK). Cell morphology was observed microscopically after 24 h incubation in the presence of varying concentrations of GGsTop. (A) 0 μM (control), (B) 5 μM, (C) 10 μM, (D) 20 μM, (E) 50 μM, (F) 1000 μM (original magnification 200×).

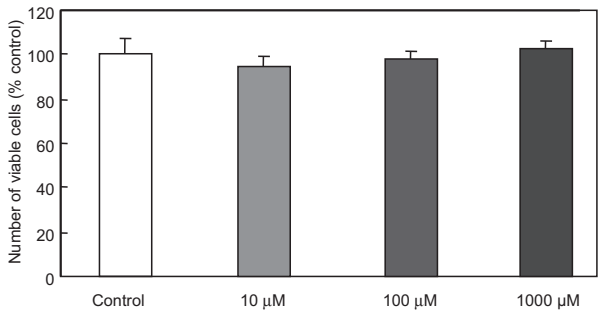

Figure 8. Effect of GGsTop on cell viability. Human skin fibroblasts (CCD-1059SK) were incubated in the presence of various concentrations of GGsTop (0, 10, 100 or 1000 μM) for 24 h. Cell viability was performed by Neutral red method (see Section 5.1).

the inhibitor GGsTop to enhance its binding (Tables 1 and 3). These results clearly support the fundamental role of Lys562 for substrate recognition (glutathione and acceptor substrate) and the inhibitor GGsTop binding. The inhibitor binding by the aid of Lys562 agrees well with our previous finding that the electrostatic interaction of GGsTop is mainly influences the initial binding of the inhibitor.[46]

Since GGsTop has a *m*-carboxymethylphenyl group in its structure, the structure is conformationally rather rigid. If the same mode of interaction with Lys562 with substrate glutathione and the acceptor substrate is supposed, their binding mode is most likely an extended conformation (Fig. 10).

Recently the crystal structure of human GGT was solved.[54,58] These structures are glutamate-bound, GGsTop-bound, and Ser-borate-bound structures. Although they gave well clear structures at the γ-glutamate binding site, little information is available for the Cys-Gly or the acceptor binding site. Since GGT is a glutathionase with significantly high transpeptidase activity, it is highly desirable to obtain the structural and mechanistic information at the Cys-Gly binding or the acceptor binding site. In this respect, GGsTop is the first inhibitor that is accessible to and well-recognized by electrostatic interaction by the active site key residue Lys562 that is most likely a key residue in recognizing the acceptor substrate as well as Cys-Gly binding of glutathione.

GGsTop is a stable compound. Based on ^{31}P NMR analysis, no hydrolysis was observed in its aqueous neutral solution for at least 28 days at ambient temperature. Further experiments indicated that GGsTop is further stable under acidic conditions (pH 1–2),

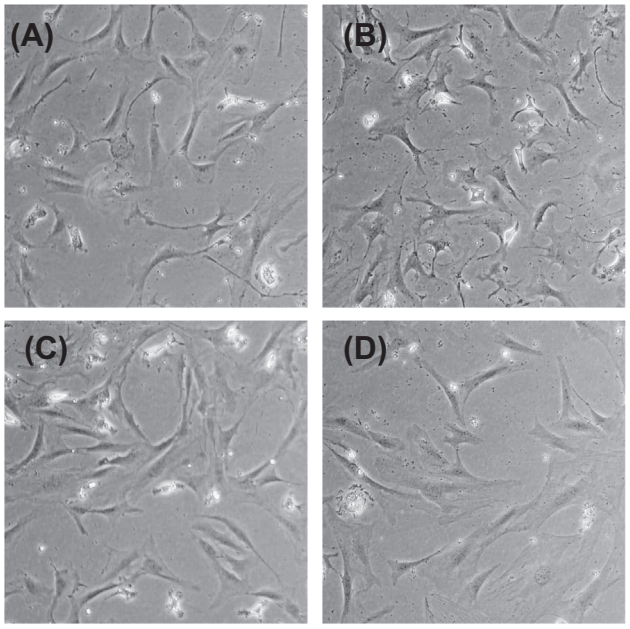

Figure 9. Effect of GGsTop on the morphology of rat hepatic stellate cells. Cell morphology was observed microscopically after 24 h incubation in the presence of various concentrations of GGsTop. (A) 0 μM (control), (B) 10 μM, (C) 100 μM, (D) 1000 μM (original magnification 200×).

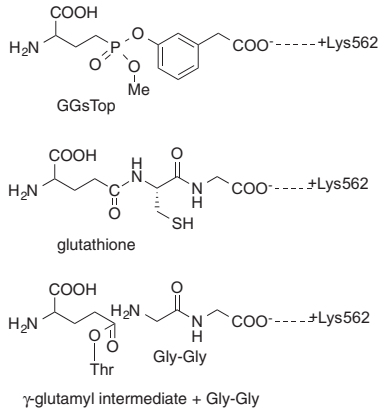

Figure 10. Proposed binding mode of GGsTop, glutathione and acceptor substrate (Gly-Gly) to Lys562.

but is not stable at >pH 8.5 where it is gradually hydrolyzed (data not shown). This is contrasted to *m*-nitrophenyl compound (**2e**), which is as active as GGsTop (Table 1), but much less stable (Fig. 6). GGsTop is an activated inhibitor towards human GGT without increasing chemical reactivity.

A thorough toxicological test of GGsTop was conducted against human cells, mammalian cells and bacteria, but no toxicity or adverse effect was observed. This may indicate that GGsTop is not incorporated into cells (negatively charged) or GGT activity is not essential for cell survival.

4. Conclusions

We demonstrated that GGsTop utilized the electrostatic interaction with the active site Lys562 of human GGT to enhance its affinity in much the same way as the acceptor substrates and Cys-Gly moiety of glutathione. The Lys562 is probably the same residue that plays the key role in transpeptidation and recognition of glutathione.

GGsTop is selective and does not inhibit glutamine amidotransferase, which might be related to its non-toxic nature. GGsTop is sufficiently stable in aqueous solution. Hence, GGsTop is an ideal GGT inhibitor for in vitro and in vivo experiments.[44,45]

5. Experimental procedures

5.1. Reagents and general methods

All reagents were obtained commercially and were used without further purification unless otherwise stated. 7-(γ-L-Glutamylamino)-4-methylcoumarin (γ-Glu-AMC) and acivicin were purchased from Sigma. γ-Glu-PNA and Gly-Gly were obtained from Wako Pure Chemical Industries. GlyMe was obtained Nacalai Tesque as a hydrochloride. Gly-GlyMe was synthesized by the esterification of Gly-Gly under acidic condition (hydrogen chloride generated from thionyl chloride and methanol). Human γ-glutamyl transpeptidase HC-GTP (T-72) was a generous gift from Asahi Kasei Corporation (Osaka, Japan), and the enzyme preparation contained a large amount of bovine serum albumin as enzyme stabilizer (GGT content <1%). *E. coli* γ-glutamyl transpeptidase was purified from the periplasmic fraction of a recombinant strain of *E. coli* K-12 (SH642) as described previously.[59,60] *E. coli* asparagine synthetase B (glutamine-hydrolyzing) (EC 6.3.5.4) was a generous gift from Professor Nigel G. J. Richards of School of Chemistry, Cardiff University, and L-glutamate dehydrogenase was purchased from Oriental Yeast Co., Ltd. The cDNA of WT human GGT was a kind gift from Professor Naoyuki Taniguchi of Osaka University.

Racemic benzyl 2-benzyloxycarbonylamino-4-(dihydroxyphosphoryl)butanoate (**4**, Z-APBA-OBn) was synthesized following the literature methods.[46] Benzyl 3-hydroxybenzoate, benzyl 3- and 4-hydroxyphenylacetate, benzyl 3-(3-hydroxyphenyl)propanoate were synthesized as described in Supplementary Contents. Ethyl 3-hydroxyphenylacetate was synthesized by the esterification of 3-hydroxyphenylacetic acid under acidic conditions (hydrogen chloride generated from thionyl chloride and ethanol), and 3-hydroxyphenylacetamide was synthesized from ethyl 3-hydroxyphenylacetate by treating 28% aqueous ammonia solution (see Supplementary Contents). Synthesis of **6f**, **6h**, **2f**, and **2h** was reported previously.[46]

^{1}H and ^{31}P NMR spectra were recorded on a JEOL JNM-AL300 (300 MHz for ^{1}H; 121 MHz for ^{31}P). Chemical shifts were recorded relative to the internal standard (tetramethylsilane for ^{1}H in $CDCl_3$) or to the external standard [sodium 3-(trimethylsilyl)propanesulfonate for ^{1}H in D_2O and 85% H_3PO_4 for ^{31}P]. Mass spectra were obtained on a JEOL JMS-700 spectrometer. Elemental analyses were performed on a Yanaco MT-5. Thin layer chromatography was carried out using silica gel plates (Merck 5715, 0.25 mm). Synthetic compounds were purified by flash column chromatography on silica gel 60N (Kanto Kagaku, spherical and neutral, 40–50 μm, No. 37563-79) or by medium-pressure reversed-phase column chromatography using a Yamazen YFLC System (Yamazen Co., Osaka, Japan) using ODS-S-50B column. UV absorbance was determined by a Shimadzu UV-3101PC.

5.2. General procedure for the preparation of 6a–h

The preparation of **6a** is representative. To a mixture of racemic Z-APBA-OBn (**4**, 1.96 g, 4.81 mmol) and *N*,*N*-dimethylformamide (1 drop) in anhydrous dichloromethane (10 mL) was added oxalyl chloride (1.7 mL, 19.8 mmol), and the mixture was stirred for 30 min at 30 °C. The volatiles were removed by flushing argon and the residue was further concentrated in vacuo. The remnant compound **5** was dissolved in anhydrous dichloromethane (40 mL) and the resulting solution was cooled to −78 °C. To the solution were added methanol (195 μL, 4.81 mmol) and triethylamine (0.74 mL, 5.31 mmol) successively. The cooling bath was removed and the mixture was further stirred for 2 h. To the mixture was added benzyl 3-hydroxybenzoate (1.21 g, 5.30 mmol) at 0 °C followed by addition of triethylamine (0.81 mL, 5.81 mmol). The mixture was stirred for 2 h at 30 °C and concentrated under reduced pressure. To the residue was added acetone and insoluble materials were removed by filtration. The filtrate was evaporated and the crude product was purified by flash column chromatography (hexane/ethyl acetate = 5:8) to give **6a** (1.49 g, 49%) as a ca. 1:1 diastereoisomeric mixture (pale yellow oil).

5.2.1. (2*RS*,$R_P$$S_P$)-Benzyl 2-benzyloxycarbonylamino-4-{[3-(benzyloxycarbonyl)phenoxy](methoxy)phosphoryl} butanoate (6a)

Yield 49%. ^{1}H NMR ($CDCl_3$) δ_H: 1.78–2.13 (3H, m), 2.21–2.38 (1H, m), 3.73 (3H, d, J = 11.1 Hz), 4.45–4.53 (1H, m), 5.10 (2H, s), 5.17 (2H, br s), 5.36 (2H, s), 5.51 (1H, br d, J = 6.9 Hz), 7.30–7.46 (17H, m), 7.80–7.92 (2H, m). ^{31}P NMR ($CDCl_3$) δ_P: 29.8. Anal. calcd for $C_{34}H_{34}NO_9P$: C, 64.65; H, 5.43; N, 2.22; found: C, 64.26; H, 5.50; N, 2.28. HRMS-FAB-NBA (m/z): $[M+H]^+$ calcd for $C_{34}H_{35}NO_9P$, 632.2049; found 632.2056.

5.2.2. (2*RS*,$R_P$$S_P$)-Benzyl 2-benzyloxycarbonylamino-4-{[3-(2-benzyloxycarbonylethyl)phenoxy](methoxy)phosphoryl} butanoate (6b)

Yield 26%, pale yellow oil. ^{1}H NMR ($CDCl_3$) δ_H: 1.77–2.13 (3H, m), 2.17–2.35 (1H, m), 2.66 (2H, t, J = 7.7 Hz), 2.94 (2H, t, J = 7.7 Hz), 3.72 (3H, d, J = 11.1 Hz), 4.44–4.51 (1H, m), 5.10 (4H,

s), 5.17 (2H, s), 5.53 (1H, br d, J = 7.5 Hz), 6.97–7.01 (3H, m), 7.20 (1H, dd, J = 8.6 and 7.7 Hz), 7.26–7.40 (15H, m). ^{31}P NMR ($CDCl_3$) δ_P: 29.2. HRMS-FAB-glycerol (m/z): $[M+H]^+$ calcd for $C_{36}H_{39}NO_9P$, 660.2362; found 660.2359.

5.2.3. (2*RS*,R_P*S*$_P$)-Benzyl 2-benzyloxycarbonylamino-4-{[3-(ethoxycarbonylmethyl)phenoxy](methoxy)phosphoryl}butanoate (6c)

Yield 55%, colorless oil: ^{1}H NMR ($CDCl_3$) δ_H: 1.23 (3H, t, J = 6.9 Hz), 1.78–2.13 (3H, m), 2.18–2.36 (1H, m), 3.58 (2H, s), 3.73 (3H, d, J = 10.8 Hz), 4.13 (2H, q, J = 6.9 Hz), 4.44–4.51 (1H, m), 5.10 (2H, s), 5.17 (2H, s), 5.62 (1H, br d, J = 4.5 Hz), 7.05–7.11 (3H, m), 7.25 (1H, dd, J = 8.0 and 8.0 Hz), 7.33 (10H, br s). ^{31}P NMR ($CDCl_3$) δ_P: 29.4. Anal. calcd for $C_{30}H_{34}NO_9P$: C, 61.74; H, 5.87; N, 2.40; found: C, 61.48; H, 6.00; N, 2.48. HRMS-FAB-glycerol (m/z): $[M+H]^+$ calcd for $C_{30}H_{35}NO_9P$, 584.2049; found 584.2039.

5.2.4. (2*RS*,R_P*S*$_P$)-Benzyl 2-benzyloxycarbonylamino-4-{[3-(carbamoylmethyl)phenoxy](methoxy)phosphoryl}butanoate (6d)

Yield 41%, colorless oil: ^{1}H NMR ($CDCl_3$) δ_H: 1.73–2.13 (3H, m), 2.18–2.34 (1H, m), 3.52 (2H, s), 3.75 (3H, d, J = 11.4 Hz), 4.43–4.50 (1H, m), 5.09 (2H, s), 5.17 (2H, s), 5.42–5.75 (3H, m), 7.06–7.11 (3H, m), 7.26–7.34 (11H, m). ^{31}P NMR ($CDCl_3$) δ_P: 29.6, 29.7 (ratio = 1:1). Anal. calcd for $C_{28}H_{31}N_2O_8P$: C, 60.65; H, 5.63; N, 5.05; found: C, 60.50; H, 5.78; N, 5.06. HRMS-FAB-NBA (m/z): $[M+H]^+$ calcd for $C_{28}H_{32}N_2O_8P$, 555.1896; found 555.1898.

5.2.5. (2*RS*,R_P*S*$_P$)-Benzyl 2-benzyloxycarbonylamino-4-[(3-nitrophenoxy)(methoxy)phosphoryl]butanoate (6e)

Yield 44%, pale yellow oil. ^{1}H NMR ($CDCl_3$) δ_H: 1.81–2.17 (3H, m), 2.22–2.39 (1H, m), 3.77 (3H, d, J = 11.1 Hz), 4.48–4.54 (1H, m), 5.11 (2H, s), 5.19 (2H, s), 5.49 (1H, br d, J = 7.8 Hz), 7.30–7.39 (10H, m), 7.46–7.56 (2H, m), 8.01–8.06 (2H, m). ^{31}P NMR ($CDCl_3$) δ_P: 30.4. HRMS-FAB-NBA (m/z): $[M+H]^+$ calcd for $C_{26}H_{28}N_2O_9P$, 543.1532; found 543.1523.

5.2.6. (2*RS*,R_P*S*$_P$)-Benzyl 2-benzyloxycarbonylamino-4-{[4-(benzyloxycarbonyl)phenoxy](methoxy)phosphoryl}butanoate (6g)

Yield 48%, colorless oil: ^{1}H NMR ($CDCl_3$) δ_H: 1.78–2.13 (3H, m), 2.22–2.35 (1H, m), 3.74 (3H, d, J = 11.1 Hz), 4.45–4.52 (1H, m), 5.08 (1H, d, J = 11.1 Hz), 5.12 (1H, d, J = 11.1 Hz), 5.15 (1H, d, J = 12.9 Hz), 5.19 (1H, d, J = 12.9 Hz), 5.35 (2H, s), 5.47 (1H, br d, J = 7.2 Hz), 7.21 (2H, d, J = 8.7 Hz), 7.28–7.45 (15H, m), 8.04 (2H, d, J = 8.7 Hz). ^{31}P NMR ($CDCl_3$) δ_P: 29.5. Anal. calcd for $C_{34}H_{34}NO_9P$: C, 64.65; H, 5.43; N, 2.22; found: C, 64.72; H, 5.54; N, 2.22. HRMS-FAB-NBA (m/z): $[M+H]^+$ calcd for $C_{34}H_{35}NO_9P$, 632.2049; found 632.2057.

5.2.7. (2*RS*,R_P*S*$_P$)-Benzyl 2-benzyloxycarbonylamino-4-{bis[3-(benzyloxycarbonylmethyl)phenoxy]phosphoryl}butanoate (7a)

To an ice cold solution of compound **5** (prepared from 10.6 mmol of racemic Z-APBA-OBn as described above) and benzyl 3-hydroxyphenylacetate (4.74 g, 19.6 mmol) in anhydrous dichloromethane (40 mL) was added triethylamine (4.0 mL, 28.7 mmol) dropwise and the mixture was stirred for 18 h at room temperature. To the reaction mixture was added silica gel (50 mL) and the volatile compounds were evaporated. The residue was subjected to silica gel flash column chromatography (hexane/ethyl acetate = 3:2) to give the title compound (6.42 g, 71%) as a pale yellow oil. ^{1}H NMR ($CDCl_3$) δ_H: 1.94–2.22 (3H, m), 2.31–2.47 (1H, m), 3.61 (4H, s), 4.47–4.54 (1H, m), 5.10 (6H, s), 5.17 (2H, s), 5.56 (1H, br d, J = 8.1 Hz), 7.03–7.08 (6H, m), 7.22 (2H, dd, J = 8.1 and 8.1 Hz), 7.26–7.37 (20H, m). ^{31}P NMR ($CDCl_3$) δ_P: 24.6. Anal Calcd for $C_{49}H_{46}NO_{11}P$: C, 68.76; H, 5.42; N, 1.64. Found: C, 68.57; H, 5.53; N, 1.64.

5.2.8. (2*RS*,R_P*S*$_P$)-Benzyl 2-benzyloxycarbonylamino-4-(diphenoxyphosphoryl)butanoate (7b)

This compound was prepared as described for **7a**. Yield 60%, colorless oil. ^{1}H NMR ($CDCl_3$) δ_H: 1.94–2.25 (3H, m), 2.33–2.48 (1H, m), 4.49–4.56 (1H, m), 5.10 (2H, s), 5.18 (2H, br s), 5.49 (1H, br d, J = 7.8 Hz), 7.10–7.34 (20H, m). ^{31}P NMR ($CDCl_3$) δ_P: 24.5. HRMS-FAB-NBA (m/z): $[M+H]^+$ calcd for $C_{31}H_{31}NO_7P$, 560.1838; found 560.1837.

5.3. General procedure for the synthesis of 2a–d, 2g, 3a, and 3b

The preparation of **2a** is representative. Hydrogen gas was bubbled into a mixture of compound **6a** (1.31 g, 2.07 mmol), water (7 mL), and acetic acid (6 mL) in the presence of 5% palladium on activated carton (0.20 g) for 4 h at room temperature. The catalyst was removed by filtration and the concentrated filtrate was lyophilized to afford **2a** (0.59 g, 90%) as a colorless solid.

5.3.1. (2*RS*,R_P*S*$_P$)-2-Amino-4-[(3-carboxyphenoxy)(methoxy)phosphoryl]butanoic acid (2a)

Yield 90%, colorless solid: ^{1}H NMR (D_2O) δ_H: 2.12–2.40 (4H, m), 3.88 (3H, d, J = 11.1 Hz), 3.89 (1H, br s), 7.46 (1H, br d, J = 8.0 Hz), 7.55 (1H, dd, J = 8.0 and 8.0 Hz), 7.77 (1H, br s), 7.89 (1H, br d, J = 8.0 Hz). ^{31}P NMR (D_2O) δ_P: 32.6. HRMS-FAB-glycerol (m/z): $[M+H]^+$ calcd for $C_{12}H_{17}NO_7P$, 318.0743; found 318.0755.

5.3.2. (2*RS*,R_P*S*$_P$)-2-Amino-4-{[3-(2-carboxyethyl)phenoxy](methoxy)phosphoryl}butanoic acid (2b)

Yield 87%, colorless solid: ^{1}H NMR (D_2O) δ_H: 2.10–2.30 (4H, m), 2.68 (2H, t, J = 7.2 Hz), 2.93 (2H, t, J = 7.2 Hz), 3.82 (1H, br s), 3.84 (3H, d, J = 11.4 Hz), 7.07 (1H, d, J = 7.5 Hz), 7.09 (1H, s), 7.17 (1H, d, J = 7.5 Hz), 7.36 (1H, dd, J = 7.5 and 7.5 Hz). ^{31}P NMR (D_2O) δ_P: 32.5. HRMS-FAB-glycerol (m/z): $[M+H]^+$ calcd for $C_{14}H_{21}NO_7P$, 346.1056; found 346.1059.

5.3.3. (2*RS*,R_P*S*$_P$)-2-Amino-4-{[3-(ethoxycarbonylmethyl)phenoxy](methoxy)phosphoryl}butanoic acid (2c)

Yield 86%, colorless solid: δ_H: 1.23 (3H, t, J = 7.2 Hz), 2.09–2.33 (4H, m), 3.75 (2H, s), 3.82 (1H, br s), 3.84 (3H, d, J = 11.1 Hz), 4.16 (2H, q, J = 7.2 Hz), 7.15–7.21 (3H, m), 7.41 (1H, dd, J = 8.0 and 8.0 Hz). ^{31}P NMR (D_2O) δ_P: 32.7. HRMS-FAB-glycerol (m/z): $[M+H]^+$ calcd for $C_{15}H_{23}NO_7P$, 360.1212; found 360.1212.

5.3.4. (2*RS*,R_P*S*$_P$)-2-Amino-4-{[3-(carbamoylmethyl)phenoxy](methoxy)phosphoryl}butanoic acid (2d)

Yield 98%, colorless solid: ^{1}H NMR (D_2O) δ_H: 2.11–2.34 (4H, m), 3.67 (2H, s), 3.85 (1H, br s), 3.88 (3H, d, J = 11.4 Hz), 7.18–7.26 (3H, m), 7.45 (1H, dd, J = 7.8 and 7.8 Hz). ^{31}P NMR (D_2O) δ_P: 32.7. HRMS-FAB-glycerol (m/z): $[M+[M+H]^+$ calcd for $C_{13}H_{20}N_2O_6P$, 331.1059; found 331.1051.

5.3.5. (2*RS*,R_P*S*$_P$)-2-Amino-4-{[3-nitrophenoxy](methoxy)phosphoryl}butanoic acid (2e)

To compound **2e** (1.09 g, 2.01 mmol) dissolved in nitromethane (10 mL) were added anisole (1.30 g, 12.0 mmol) and aluminum chloride (0.80 g, 6.00 mmol) successively, and the mixture was stirred for 3 h at ambient temperature. When the reaction was complete, water (20 mL) was added and the mixture was washed with diethyl ether (3 × 50 mL). The mixture was passed through the silica gel column (eluted with MeOH) and the red fraction was collected. The fractions were evaporated and purified by ODS column (30–60% MeOH/H_2O, eluted at 60% MeOH). Lyophilization gave **2e** as colorless solid. Yield 0.40 g (63%). ^{1}H NMR (D_2O) δ_H: 2.17–2.42 (4H, m), 3.86 (1H, br s), 3.88 (3H, d, J = 12.0 Hz), 7.62–7.68 (2H, m), 8.04–8.14 (2H, m). ^{31}P NMR (D_2O)

δ_P: 32.9. HRMS-FAB-glycerol (m/z): $[M+H]^+$ calcd for $C_{11}H_{16}N_2O_7P$, 319.0695; found 319.0694.

5.3.6. (2*RS*,*R*$_P$*S*$_P$)-2-Amino-4-[(4-carboxyphenoxy)(methoxy) phosphoryl]butanoic acid (2g)

Yield 88%, colorless solid: ^{1}H NMR (D_2O) δ_H: 2.13–2.41 (4H, m), 3.87 (1H, br s), 3.89 (3H, d, J = 11.4 Hz), 7.32 (2H, d, J = 8.1 Hz), 8.05 (2H, d, J = 8.1 Hz). ^{31}P NMR (D_2O) δ_P: 32.4. HRMS-FAB-NBA (m/z): $[M+H]^+$ calcd for $C_{12}H_{17}NO_7P$, 318.0743; found 318.0747.

5.3.7. (2*RS*,*R*$_P$*S*$_P$)-2-Amino-4-{bis[(3-carboxymethy)lphenoxy] phosphoryl}butanoic acid (3a)

The crude product was purified by ODS column and lyophilized. Yield 71%, colorless solid. ^{1}H NMR (D_2O) δ_H: 2.30–2.57 (4H, m), 3.65 (4H, s), 3.89 (1H, br s), 6.98 (2H, br s), 7.07 (2H, br d, J = 7.8 Hz), 7.16 (2H, br d, J = 7.8 Hz), 7.35 (2H, dd, J = 7.8 and 7.8 Hz). ^{31}P NMR (D_2O) δ_P: 28.1. HRMS-FAB-glycerol (m/z): $[M+H]^+$ calcd for $C_{20}H_{23}NO_9P$, 452.1110; found 452.1112.

5.3.8. (2*RS*,*R*$_P$*S*$_P$)-2-Amino-4-(diphenoxyphosphoryl)butanoic acid (3b)

The crude product was purified by ODS column and lyophilized. Yield 61%, colorless solid. ^{1}H NMR (D_2O) δ_H: 2.30–2.53 (4H, m), 3.84–3.90 (1H, m), 7.19 (4H, d, J = 7.5 Hz), 7.31 (2H, dd, J = 7.5 and 7.5 Hz), 7.44 (4H, dd, J = 7.5 and 7.5 Hz). ^{31}P NMR (D_2O) δ_P: 28.3. HRMS-FAB-glycerol (m/z): $[M+H]^+$ calcd for $C_{16}H_{19}NO_5P$, 336.1001; found 336.1001.

5.4. Enzyme activity and time-dependent inhibition assay of GGT

The hydrolytic activity of human and *E. coli* GGT were measured as described in our previous papers using γ-Glu-AMC as a substrate.[46,49]

5.5. Glutaminase assay for the glutaminase activity of *E. coli* asparagine synthetase B

For the glutaminase activity, we use the L-glutamate dehydrogenase assay that monitors the production of NADH from NAD^+ while glutamate is converted to α-ketoglutarate and ammonia. In this assay, 100 mM EPPS buffer, pH 8, 20 mM L-Gln (purified by crystallization before use), 100 mM NaCl, 8 mM $MgCl_2$, 0.5 mM DTT, were all premixed to a total volume of 200 μL. Glutminase-asparagine synthetase B (1–3 μg) was added, and the mixture was incubated at 37 °C for 10 min and then quenched with 30 μL 20% TCA. This was done in the presence and absence of inhibitor. The entire mixture is added to a cuvette containing 770 μL of 300 mM glycine–250 mM hydrazine buffer, pH 9, 1 mM ADP, and 1.5 mM NAD^+, for a total reaction volume of 1 mL. This was mixed thoroughly and 2.2 U of L-glutamate dehydrogenase (Sigma) was added to initiate the reaction. Absorbance was monitored at 340 nm for 30 min and the difference between the final and initial measurements were compared to that of a set of glutamate standards.

5.6. Inhibition of glutaminase activity of asparagine synthetase B by acivicin and GGsTop

The asparagine synthetase (60 μg) was incubated at 30 °C for 120 min in a total volume of 60 μL of 100 mM Tris–HCl buffer (pH 7.5) containing 8 mM $MgCl_2$, 100 mM NaCl and 0.5 mM DTT in the presence or the absence of varying concentrations 0.1 mM of acivicin and varying concentration of GGsTop (0.1, 1 and 10 mM). An aliquot of 20 μL of the solution was withdrawn after 30 and 120 min for assay for the residual glutaminase activity.

5.7. X-ray crystallography of *E. coli* GGT in complex with inhibitor 1

The expression, purification and crystallization of *E. coli* GGT were described previously.[59,60] Inhibitor-bound crystals were prepared by soaking crystals for several minutes in a crystallization solution containing 5 mM **1**. The crystals were soaked in cryoprotectant solution, which was prepared by adding PEG 4000 and glycerol to the reservoir solution to final concentrations of 22.5% (w/v) and 15% (v/v), respectively and flash-cooled with a nitrogen gas stream at 100 K. Diffraction data for **1**-bound GGT crystal were collected using synchrotron radiation and the Jupiter 210 detector (RIGAKU) in beamline BL38B1 at SPring-8 (Harima, Japan). Diffraction images were processed and integrated intensities were merged and scaled using the XDS.[61] Results of the data collection are summarized in Table 2.

Because the inhibitor-bound GGT crystals were nearly isomorphous with the native GGT crystal, the structure of **1**-bound GGT was determined using the structure of the native GGT (PDB ID: 2DBU). Rigid-body, simulated annealing and temperature-factor refinements using PHENIX[62] were applied to the model. COOT[63] was used to revise the structure. In this step, the inhibitor was clearly visible in the electron density map. After one cycle of water picking and conjugate gradient energy minimization refinement, and temperature-factor refinements, the model of the inhibitor was fitted to the $F_o - F_c$ map in the substrate-binding pocket. Finally, conjugate gradient energy minimization and temperature-factor refinements were applied to the model including the inhibitor. Refinement statistics are summarized in Table 2. Coordinates and structure factors have been deposited in the RCSB Protein Data Bank with accession code 5B5T.

All structure figures were prepared with PyMOL,[64] and the electrostatic potentials of the molecular surface were calculated with PBEQ-solver,[65] which uses the Poisson–Boltzmann equations module from the biomolecular simulation program CHARMM.[66]

5.8. Preparation of the recombinant baculovirus for expression of GGT

The cDNA of WT human GGT (N-terminal truncated) was kindly provided by Professor Naoyuki Taniguchi of Osaka University. Human GGT is a membrane-bound enzyme in which the amino-terminal signal sequence functions as a membrane-anchoring domain, and deletion of the signal peptide (1–27 amino acid residues) resulted in the secretion of a soluble and active glycosylated protein into the medium when expressed in insect cells using a baculovirus system.[56] The cDNA encoding human GGT with the deletion of 1–27 residues at the amino-terminus was amplified with a set of primers: hGGT-del27N (*Eco*RI), GAATTCATGGCCTCCAAGGAACCTGACAACC, and hGGT-C (*Xho*I), CTCGAGTCAGTAGCCGGCAGGCTCCCC, and the DNA fragment digested with *Eco*RI and *Xho*I was ligated into the pFastBac1 vector (Invitrogen). The recombinant Bacmid DNA was prepared with an *Escherichia coli* strain DH10Bac according to a mamufacture's instruction (Invitrogen). To prepare the expression plasmid for the K562S mutant of human GGT, site-directed mutagenesis was performed with a primer of hGGT_K562S, CTCGAGTCAGTAGCCGGCAGGCTCCCCGCCTGACCTGGAGTCCGAGGC by a QuickChange site-directed mutagenesis kit (Stratagene). Preparation of the recombinant baculovirus DNA and transfection of insect cells were carried out according to the instructions of the manufacture (Invitrogen).

5.9. Expression of GGT by insect cells

Wild type and K562S mutant human GGT were expressed by insect cells in glutamine-supplemented medium as follow: Express

Five SFM was supplemented with 10% (v/v) 200 mM L-glutamine. Suspension cultures (75 mL) of *Trichoplusia ni* BTI-Tn-5B1-4 (High Five™) cells were infected with the recombinant baculovirus and incubated in a 300 mL Erlenmeyer flask for 4 d in a rotary shaker at 27 °C at 150 rpm.

5.10. Measurement of GGT activity

The activity of GGT was measured under the standard transpeptidation assay method[67] as follows: The reaction was initiated by adding an enzyme solution to 100 mM Tris–HCl buffer (pH 8.0) containing 1 mM γ-Glu-PNA as a donor substrate and 20 mM Gly-Gly as an acceptor to a total volume of 1 mL in a spectrometer cuvette at 37 °C. The rate of release of *p*-nitroaniline was recorded continuously at 410 nm ($\varepsilon = 8800\ M^{-1}\ cm^{-1}$) for 1 min. One unit of enzyme is defined as the amount of the enzyme that releases 1 mmol of *p*-nitroaniline in 1 min at 37 °C. The transpeptidation activities for Gly-GlyMe and GlyMe were measured by the same method as described above with respective acceptors (20 mM each). A stock solution of 100 mM Gly-Gly, Gly-GlyMe and GlyMe (pH adjusted to 8.0 with aq NaOH) was used for the transpeptidation assay. The hydrolytic activity was measured without adding the accepter substrate under the same reaction conditions.

5.11. Purification of WT human GGT

Suspension cultures of the infected High Five™ cells were centrifuged at 2330×*g* for 15 min, and the supernatant was harvested. The supernatant was applied directly to a Con A Sepharose column (16 × 60 mm) (GE Healthcare, Buckinghamshire, England) equilibrated with 10 mM sodium phosphate buffer (pH 6.5). After the column was washed with the same buffer (60 mL), the protein was eluted with a buffer containing 1 mM α-methyl-D-mannopyranoside at a flow rate of 0.2 mL/min. The active fractions were combined, and the pH of the solution was adjusted to 8.0 by addition of 1 M Tris–HCl buffer (pH 8.0). The solution was applied to a Q Sepharose column (26 × 90 mm) (GE Healthcare) equilibrated with 20 mM Tris–HCl buffer (pH 8.0). The column was washed with the equilibration buffer and was eluted with 100 mM NaCl at a flow rate of 1 mL/min. The active fractions were combined and concentrated to ca. 4 mL by ultrafiltration (Amicon Ultra-15 30,000 MWCO, Millipore). The solution was applied to a Sephacryl™ S-200 HR (16 × 600 mm) (Amersham Biosciences, Uppsala, Sweden) gel filtration column equilibrated with 50 mM Tris–HCl buffer (pH 8.0) containing 150 mM NaCl and was eluted with the equilibration buffer. The active fractions were pooled and was analyzed with SDS–PAGE.

5.12. Purification of K562S mutant of human GGT

The suspension cultures of the infected High Five™ cells were centrifuged at 2330×*g* for 15 min, and the supernatant was harvested. The supernatant was applied directly to a Con A Sepharose column (16 × 60 mm) (GE Healthcare, Buckinghamshire, England) equilibrated with 10 mM sodium phosphate buffer (pH 6.5). After washing the column with the same buffer (60 mL), the protein was eluted with a buffer containing 1 mM α-methyl-D-mannopyranoside at a flow rate of 0.2 mL/min. The active fractions were pooled. One mM Tris–HCl buffer (pH 8.0, 8 mL) was added to the Con A elute of K562S mutant protein (88 mL), and the resulting mixture was incubated at 37 °C for 8 h for autocatalytic processing. The solution of the processed K562S mutant was applied to a Q Sepharose column (26 × 90 mm) (GE Healthcare) equilibrated with 20 mM Tris–HCl buffer (pH 8.0). The column was washed with the equilibration buffer and was eluted with a liner gradient of NaCl from 20 to 250 mM at a flow rate of 1 mL/min. The active fractions were combined and concentrated to ca. 4 mL by ultrafiltration (Amicon Ultra-15 30,000 MWCO, Millipore).

5.13. Toxicity test for cultured cells

Normal human skin fibroblasts (CCD-1059SK) were purchased from DS Pharma Biomedical Co., Ltd (Osaka, Japan). Skin fibroblasts were cultured in 25 cm^2 tissue culture flask (Greiner Bio-One, Frickenshausen, Germany) with Dulbecco's modified Eagle Medium (DMEM) (Nissui Pharmaceutical Co., Ltd, Tokyo, Japan) containing 10% FBS supplemented with antibiotics (10^5 U/L of penicillin G and 500 mg/L of streptomycin). Cells were incubated in a humidified atmosphere of 5% CO_2 in air at 37 °C. When the cells reached confluence, they were detached with 0.025% trypsin/0.01% EDTA. Skin fibroblasts of passages 10–20 were used in all experiments. Cells were plated at 3×10^4 cells/mL on Chamber slide (Nalge Nunc International, New York, USA) with DMEM containing 10% FBS. After 24 h of pre-incubation of the cells, GGsTop (0, 5, 10, 20, 50 or 1000 μM) was dissolved in distilled water and diluted in the DMEM immediately before use. In all the experiments, control cultures were made up of the medium, distilled water and the cells. The cells were incubated for 24 h. At the end of incubation, the cell morphology was observed under the inverted microscope (IX-70, OLYMPUS, Co., Ltd, Tokyo, Japan). Cell viability was measured by the Neutral Red assay, as described previously.[68] Rat hepatic stellate cells (HSCs) were isolated from male Wistar rats weighing 300–350 g, as previously described.[69] The HSCs were identified by their typical star-like configuration and vitamin A autofluorescence. The purity was always greater than 95%. The cells were plated on 35 mm plastic dishes at a density of 5×10^5 cells/ml in 1.5 ml of DMEM containing 10% FBS supplemented with antibiotics (105 U/l penicillin G and 500 mg/l streptomycin) for 2 days and then cultured in fresh medium without serum for 24 h in a humidified atmosphere (5% CO_2/95% air) at 37 °C. After pre-incubation, the cells were cultured in DMEM with different concentrations of GGsTop (0, 10, 100 or 1000 μM). The cells were incubated for 24 h. At the end of incubation, the cell morphology was observed under the inverted microscope (IX-70, OLYMPUS, Co., Ltd, Tokyo, Japan).

AMES test and in vitro cell growth inhibition and chromosome aberration test was conducted by Biotoxtech Co., Ltd through Iwase Cosfa Co. Ltd.

Acknowledgments

We thank Asahi Kasei Corporation for the generous gift of human GGT (HC-GTP). We also thank Professor Nigel G. J. Richards of School of Chemistry, Cardiff University, for the generous gift of *E. coli* asparagine synthetase B (glutamine-hydrolyzing). We also thank Professor Naoyuki Taniguchi of Osaka University for the generous gift of the cDNA of WT human GGT. This study was supported in part by JSPS KAKENHI Grant Number JP19310143 (J.H.). The HRMS in this study was obtained with the JMS-700 spectrometer in the Joint Usage/Research Center (JURC) at Institute for Chemical Research, Kyoto University.

A. Supplementary data

Supplementary data associated with this article can be found, in the online version, at http://dx.doi.org/10.1016/j.bmc.2016.08.050.

References and notes

1. Whitfield, J. B. *Crit. Rev. Clin. Lab. Sci.* **2001**, *38*, 263.
2. Keillor, J. W.; Castonguay, R.; Lherbet, C. *Methods Enzymol.* **2005**, *401*, 449.

3. Keillor, J. W.; Ménard, A.; Castonguay, R.; Lherbet, C.; Rivard, C. *J. Phys. Org. Chem.* **2004**, *17*, 529.
4. Allison, R. D. *Methods Enzymol.* **1985**, *113*, 419.
5. Hiratake, J.; Suzuki, H.; Fukuyama, K.; Wada, K.; Kumagai, H. In *Handbook of Proteolytic Enzymes*; Rawlings, N. D., Salvesen, G., Eds., 3rd ed.; ; Academic Press: Oxford, 2013; Vol. 3, pp 3712–3719.
6. Robert de Saint Vincent, B.; Mousset, S.; Jacquemin-Sablon, A. *Eur. J. Biochem.* **1999**, *262*, 873.
7. Ruoso, P.; Hedley, D. W. *Cancer Chemother. Pharmacol.* **2004**, *54*, 49.
8. Zhang, H.; Forman, H. J.; Choi, J. *Methods Enzymol.* **2005**, *401*, 468.
9. Taniguchi, N.; Ikeda, Y. *Adv. Enzymol. Relat. Areas Mol. Biol.* **1998**, *72*, 239.
10. Lieberman, M. W.; Barrios, R.; Carter, B. Z.; Habib, G. M.; Lebovitz, R. M.; Rajagopalan, S.; Sepulveda, A. R.; Shi, Z.-Z.; Wan, D.-F. *Am. J. Phathol.* **1995**, *147*, 1175.
11. McIntyre, T. M.; Curthoys, N. P. *J. Biol. Chem.* **1979**, *254*, 6499.
12. Curthoys, N. P.; Hughey, R. P. *Enzyme* **1979**, *24*, 383.
13. Hanigan, M. H. *Adv. Cancer Res.* **2014**, *122*, 103.
14. Hanigan, M. H.; Ricketts, W. A. *Biochemistry* **1993**, *32*, 6302.
15. Hanigan, M. H.; Frierson, H. F., Jr.; Swanson, P. E.; De Yong, B. R. *Hum. Pathol.* **1999**, *30*, 300.
16. Schäfer, C.; Fels, C.; Brucke, M.; Holzhausen, H.-J.; Bahn, H.; Wellman, M.; Visvikis, A.; Fischer, P.; Rainov, N. G. *Acta Oncol.* **2001**, *40*, 529.
17. Grimm, C.; Hofstetter, G.; Aust, S.; Mutz-Dehbalaie, I.; Bruch, M.; Heinze, G.; Rahhal-Schupp, J.; Reinthaller, A.; Concin, N.; Polterauer, S. *Br. J. Cancer* **2013**, *109*, 610.
18. Hanigan, M. H. *Carcinogenesis* **1995**, *16*, 181.
19. Corti, A.; Franzini, M.; Paolicchi, A.; Pompella, A. *Anticancer Res.* **2010**, *30*, 1169.
20. Hanigan, M. H.; Gallagher, B. C.; Townsend, D. M.; Gabarra, V. *Carcinogenesis* **1999**, *20*, 553.
21. Komlosh, A.; Volohonsky, G.; Porat, N.; Tuby, C.; Bluvshtein, E.; Steinberg, P.; Oesch, F.; Stark, A. A. *Carcinogenesis* **2001**, *22*, 2009.
22. Godwin, A. K.; Meister, A.; O'Dwyer, P. J.; Huang, C. S.; Hamilton, T. C.; Anderson, M. E. *Proc. Natl. Acad. Sci. U.S.A.* **1992**, *89*, 3070.
23. Pompella, A.; De Tata, V.; Paolicchi, A.; Zunino, F. *Biochem. Pharmacol.* **2006**, *71*, 231.
24. Obrador, E.; Carretero, J.; Ortega, A.; Medina, I.; Rodilla, V.; Pellicer, J. A.; Estrela, J. M. *Hepatology* **2002**, *35*, 74.
25. Benlloch, M.; Ortega, A.; Ferrer, P.; Segarra, R.; Obrador, E.; Asensi, M.; Carretero, J.; Estrela, J. M. *J. Biol. Chem.* **2005**, *280*, 6950.
26. Sian, J.; Dexter, D. T.; Lees, A. J.; Daniel, S.; Jenner, P.; Marsden, C. D. *Ann. Neurol.* **1994**, *36*, 356.
27. Dringen, R.; Pfeiffer, B.; Hamprecht, B. *J. Neurosci.* **1999**, *19*, 562.
28. Chinta, S. J.; Kumar, J. M.; Zhang, H.; Forman, H. J.; Andersen, J. K. *Free Radical Biol. Med.* **2006**, *40*, 1557.
29. Lee, D.-H.; Ha, M.-H.; Kim, J.-H.; Christiani, D. C.; Gross, M. D.; Steffes, M.; Blomhoff, R.; Jacobs, D. R., Jr. *Diabetologia* **2003**, *46*, 359.
30. Meisinger, C.; Löwel, H.; Heier, M.; Schneider, A.; Thorand, B. J. *Internal Med.* **2005**, *258*, 527.
31. Ruttmann, E.; Brant, L. J.; Concin, H.; Diem, G.; Rapp, K.; Ulmer, H. *Circulation* **2005**, *112*, 2130.
32. Lee, D.-H.; Silventoinen, K.; Hu, G.; Jacobs, D. R., Jr.; Jousilahti, P.; Sundvall, J.; Tuomilehto, J. *Eur. Heart J.* **2006**, *27*, 2170.
33. Kengne, A. P.; Czernichow, S.; Stamatakis, E.; Hamer, M.; Batty, G. D. *J. Hepatol.* **2012**, *57*, 1083.
34. Mason, J. E.; Starke, R. D.; Van Kirk, J. E. *Prev. Cardiol.* **2010**, *13*, 36.
35. Lowry, M. H.; McAllister, B. P.; Jean, J.-C.; Brown, L. A. S.; Hughey, R. P.; Cruikshank, W. W.; Amar, S.; Lucey, E. C.; Braun, K.; Johnson, P.; Wight, T. N.; Joyce-Brady, M. *Am. J. Respir. Cell Mol. Biol.* **2008**, *38*, 509.
36. Mistry, D.; Stockley, R. A. *COPD* **2010**, *7*, 285.
37. Stark, A.-A.; Zeiger, E.; Pagano, D. A. *Carcinogenesis* **1993**, *14*, 183.
38. Glass, G. A.; Stark, A.-A. *Environ. Mol. Mutagen.* **1997**, *29*, 73.
39. Paolicchi, A.; Minotti, G.; Tonarelli, P.; Tongiani, R.; De Cesare, D.; Mezzetti, A.; Dominici, S.; Comporti, M.; Pompella, A. J. *Invest. Med.* **1999**, *47*, 151.
40. Dominici, S.; Paolicchi, A.; Lorenzini, E.; Maellaro, E.; Comporti, M.; Pieri, L.; Minotti, G.; Pompella, A. *BioFactors* **2003**, *17*, 187.
41. Lee, D.-H.; Blomhoff, R.; Jacobs, D. R., Jr. *Free Radical Res.* **2004**, *38*, 535.
42. Dominici, S.; Paolicchi, A.; Corti, A.; Maellaro, E.; Pompella, A. *Methods Enzymol.* **2005**, *401*, 484.
43. Paolicchi, A.; Emdin, M.; Passino, C.; Lorenzini, E.; Titta, F.; Marchi, S.; Malvaldi, G.; Pompella, A. *Atherosclerosis* **2006**, *186*, 80.
44. Tuzova, M.; Jean, J.-C.; Hughey, R. P.; Brown, L. A. S.; Cruikshank, W. W.; Hiratake, J.; Joyce-Brady, M. *Front. Phramacol.* **2014**, *5*, 179. http://dx.doi.org/10.3389/fphar.2014.00179.
45. Yamamoto, S.; Watanabe, B.; Hiratake, J.; Tanaka, R.; Ohkita, M.; Matsumura, Y. *J. Pharmacol. Exp. Ther.* **2011**, *339*, 945.
46. Han, L.; Hiratake, J.; Kamiyama, A.; Sakata, K. *Biochemistry* **2007**, *46*, 1432.
47. Nakajima, M.; Watanabe, B.; Han, L.; Shimizu, B.; Wada, K.; Fukuyama, K.; Suzuki, H.; Hiratake, J. *Bioorg. Med. Chem.* **2014**, *22*, 1176.
48. Hu, X.; Legler, P. M.; Khavrutskii, I.; Scorpio, A.; Compton, J. R.; Robertson, K. L.; Friedlander, A. M.; Wallqvist, A. *Biochemistry* **2012**, *51*, 1199.
49. Han, L.; Hiratake, J.; Tachi, N.; Suzuki, H.; Kumagai, H.; Sakata, K. *Bioorg. Med. Chem.* **2006**, *14*, 6043.
50. Jayaram, H. N.; Cooney, D. A.; Ryan, J. A.; Neil, G.; Dion, R. L.; Bono, V. H. *Cancer Chemother. Rep.* **1975**, *59*, 481.
51. O'Dwyer, P. J.; Alonso, M. T.; Leyland-Jones, B. *J. Clin. Oncol.* **1984**, *2*, 1064.
52. Ahluwalia, G. S.; Grem, J. L.; Hao, Z.; Cooney, D. A. *Pharmacol. Ther.* **1990**, *46*, 243.
53. Wada, K.; Hiratake, J.; Irie, M.; Okada, T.; Yamada, C.; Kumagai, H.; Suzuki, H.; Fukuyama, K. *J. Mol. Biol.* **2008**, *380*, 361.
54. Terzyan, S. S.; Burgett, A. W. G.; Heroux, A.; Smith, C. A.; Mooers, B. H.; Hanigan, M. H. *J. Biol. Chem.* **2015**, *290*, 17576.
55. Okada, T.; Suzuki, H.; Wada, K.; Kumagai, H.; Fukuyama, K. *Proc. Natl. Acad. Sci. U.S.A.* **2006**, *103*, 6471.
56. Ikeda, Y.; Fujii, J.; Taniguchi, N.; Meister, A. *Proc. Natl. Acad. Sci. U.S.A.* **1995**, *92*, 126.
57. Suzuki, H.; Kumagai, H. *J. Biol. Chem.* **2002**, *277*, 43536.
58. West, M. B.; Chen, Y.; Wickham, S.; Heroux, A.; Cahill, K.; Hanigan, M. H.; Mooers, B. H. M. *J. Biol. Chem.* **2013**, *288*, 31902.
59. Suzuki, H.; Kumagai, H.; Echigo, T.; Tochikura, T. *Biochem. Biophys. Res. Commun.* **1988**, *150*, 33.
60. Suzuki, H.; Kumagai, H.; Tochikura, T. *J. Bacteriol.* **1986**, *168*, 1325.
61. Kabsch, W. *Acta Crystallogr., D: Biol. Crystallogr.* **2010**, *66*, 133.
62. Adams, P. D.; Afonine, P. V.; Bunkoczi, G.; Chen, V. B.; Davis, I. W.; Echols, N.; Headd, J. J.; Hung, L.-W.; Kapral, G. J.; Grosse-Kunstleve, R. W.; McCoy, A. J.; Moriarty, N. W.; Oeffner, R.; Read, R. J.; Richardson, D. C.; Richardson, J. S.; Terwilliger, T. C.; Zwart, P. H. *Acta Crystallogr., D: Biol. Crystallogr.* **2010**, *66*, 213.
63. Emsley, P.; Lohkamp, B.; Scott, W. G.; Cowtan, K. *Acta Crystallogr. D Biol. Crystallogr.* **2010**, *66*, 486.
64. DeLano, W. L. *The PyMOL Molecular Graphics System*, on World Wide Web, 2002, http://www.pymol.org.
65. Jo, S.; Kim, T.; Iyer, V. G.; Im, W. *J. Comput. Chem.* **2008**, *29*, 1859.
66. Brooks, B. R.; Brooks, C. L.; Mackerell, A. D.; Nilsson, L.; Petrella, R. J.; Roux, B.; Won, Y.; Archontis, G.; Bartels, C.; Boresch, S.; Caflisch, A.; Caves, L.; Cui, Q.; Dinner, A. R.; Feig, M.; Fischer, S.; Gao, J.; Hodoscek, M.; Im, W.; Kuczera, K.; Lazaridis, T.; Ma, J.; Ovchinnikov, V.; Paci, E.; Pastor, R. W.; Post, C. B.; Pu, J. Z.; Schaefer, M.; Tidor, B.; Venable, R. M.; Woodcock, H. L.; Wu, X.; Yang, W.; York, D. M.; Karplus, M. *J. Comput. Chem.* **2009**, *30*, 1545.
67. Meister, A.; Tate, S. S.; Griffith, O. W. *Methods Enzymol.* **1981**, *77*, 237.
68. Zhang, S.-Z.; Lipsky, M. M.; Trump, B. F.; Hsu, I.-C. *Cell Biol. Toxicol.* **1990**, *6*, 219.
69. Kojima-Yuasa, A.; Ohkita, T.; Yukami, K.; Ichikawa, H.; Takami, N.; Nakatani, T.; Kennedy, D. O.; Nishiguchi, S.; Matsui-Yuasa, I. *Chem. Biol. Interact.* **2003**, *146*, 89.